Pis'ma v ZhETF, vol. 80, iss. 9, pp. 714 – 718 

# Observation of Hubbard bands in $\gamma$-manganese

*S. Biermann*[1)], *A. Dallmeyer, C. Carbone, W. Eberhardt, C. Pampuch*[+], *O. Rader*[+], *M. I. Katsnelson*[*], *A. I. Lichtenstein*[*2)]

*Institut für Festkörperforschung, Forschungszentrum Jülich, D-52425 Jülich, Germany*

[+]*BESSY, D-12489 Berlin, Germany*

[*]*University of Nijmegen, NL-6525 ED Nijmegen, The Netherlands*

Submitted 13 October 2004

We present angle-resolved photoemission spectra of the $\gamma$-phase of manganese as well as a theoretical analysis using a recently developed approach that combines density functional and dynamical mean field methods (LDA+DMFT). The comparison of experimental data and theoretical predictions allows us to identify effects of the Coulomb correlations, namely the presence of broad and nondispersive Hubbard bands in this system.

PACS: 71.15.Qe, 71.20.Be, 79.60.–i

The electronic theory of metals is based on the concept of quasiparticles, elementary excitations in the many-electron system that show a one-to-one correspondence with non-interacting electrons. However, strong electronic correlations can destroy this picture and result in the formation of so-called Hubbard bands of essentially many-body nature [1]. This concept is crucial for modern theories of strongly correlated electron systems [2]. The formation of Hubbard bands takes place, e.g., in many transition metal-oxide compounds, which thus have to be viewed as Mott insulators or doped Mott insulators [3]. Transition metals represent another class of systems where many-body effects are important (see [4] and Refs. therein). However, according to common belief, they are moderately correlated systems and normal Fermi liquids.

Electronic spectra of transition metals have been probed intensively by angle-resolved photoemission, a technique that allows for the determination of the dispersion law that describes the dependence of the quasiparticle energy on quasimomentum. Copper was the first metal to be investigated thoroughly by this technique and the results were in excellent agreement with band structure calculations [5, 6]. The same technique, however, showed substantial deviations when applied to Ni and provided evidence for many-body behavior, such as the famous 6 eV satellite [7, 8]. The quasiparticle damping in iron can be as large as 30 % of the binding energy [9, 10]. Correlation effects are indeed important for metals with partially filled $3d$ bands and should be taken into account for an adequate description of ARPES spectra. Nevertheless, the main part of the spectral density in Fe is related to usual quasiparticles, and the spectral weight of the satellite in Ni amounts to only 20% [10]. In the present letter, we provide evidence for surprisingly strong correlation effects in the fcc-($\gamma$) phase of manganese, which are much stronger than in other transition metals.

Investigations of an extended Hubbard model show that correlation effects are strongest for half-filled $d$-bands [11]. Normally the geometrical frustrations in crystals (such as in the fcc-lattice) further enhance electronic correlations [2] so that one of the best candidates among the transition metals for the search of strong correlation effects is the fcc-($\gamma$) phase of manganese. It is an example of a very strongly frustrated magnetic system; according to band-structure calculations [12] the antiferromagnetic ground state of $\gamma$-Mn lies extremely close to the boundary of the non-magnetic phase. Moreover, an anomalously low value of the bulk modulus [13] might be considered as a first experimental hint of strong electronic correlations.

The physical properties of bulk $\gamma$-Mn are hardly accessible in the experiment, since the $\gamma$-phase is only stable at temperatures between 1368 K and 1406 K, where it shows paramagnetic behavior. Thin films of $\gamma$-Mn, however, can be stabilized by epitaxial growth on $Cu_3Au(100)$ [14], which has an interatomic spacing (2.65 Å) very close to the interatomic spacing of Mn-rich alloys (2.60–2.68 Å). Schirmer et al. [14] have shown that $Cu_3Au(100)$ supports layer-by-layer growth at room temperature up to coverages of 20 monoatomic layers (ML). A low-energy electron diffraction (LEED) I(V) analysis revealed that the Mn films adopt the in-plane spacing of the $Cu_3Au(100)$ substrate and a com-

[1)] e-mail: biermann@cpht.polytechnique.fr
[2)] e-mail: A.Lichtenstein@sci.kun.nl

paratively large tetragonal distortion of the fcc-lattice. For the inner layers of a 16 ML Mn film, this distortion amounts to -6%, whereas the surface-subsurface distance is very close to the $Cu_3Au$ value.

We have used angle-resolved photoemission at the undulator beamline TGM-5 and on the TGM-1 beamline at BESSY at a combined energy resolution of 250 meV to probe the electronic states in γ-Mn. The $Cu_3Au(100)$ substrate was prepared by repeated cycles of $Ne^+$ sputtering and annealing, until a very good LEED pattern with sharp diffraction spots and a low background intensity confirmed a high degree of structural order. The base pressure of $2 \cdot 10^{-10}$ mbar rose to $7 \cdot 10^{-10}$ mbar as Mn was deposited by electron beam evaporation. To avoid interdiffusion of Cu and Au, the onset of which was determined to be above room temperature [14] we used to keep the sample at room temperature during the Mn deposition and the photoemission measurements. We observe in all experiments LEED patterns of $Mn/Cu_3Au$ of $(1\times1)$ type and a quality comparable to those of Fig.3 of Ref. [15].

Angle-resolved photoemission measures the electron spectral density $A(\mathbf{k}, E)$ as a function of the quasimomentum $\mathbf{k}$ and the energy $E$ multiplied by the Fermi distribution function $f(E)$ [16]. For a given photon energy and electron emission angle corresponding to a certain $\mathbf{k}$ in the photoemission initial state, the spectral density usually has a well-defined maximum as a function of $E$ that determines the quasiparticle dispersion $E(\mathbf{k})$ for the occupied part of the electronic bands. Figure 1 shows experimental data obtained for γ-Mn at a photon energy of 34 eV. This energy was chosen to follow the [111]-direction ($\Gamma-L$) as closely as possible starting out near Γ at 0° and reaching $L$ around 30° electron emission angle. The spectra are characterized by two striking features. These are a weakly dispersive quasiparticle band near the Fermi level $E_F$ and a broad and almost $\mathbf{k}$-independent maximum at approximately 2.7 eV below $E_F$. These structures lack a significant dispersion also in spectra taken at normal electron emission corresponding to the [100]-direction for photon energies from 14 eV ($\sim 0.3\overline{\Gamma X}$) to 70 eV ($\sim 0.5\overline{X\Gamma}$) in Fig.2.

These data cannot be understood in the framework of a standard quasiparticle picture, since first principles calculations of the band structure for different magnetic phases of γ-Mn show an energy dispersion of more than 1.5 eV [17] (Fig.4). Instead, the overall shape of the experimental spectra is very close to that of the Hubbard model on the metallic side of the Mott transition with a quasiparticle band near the Fermi level and a broad Hubbard band below $E_F$ [18].

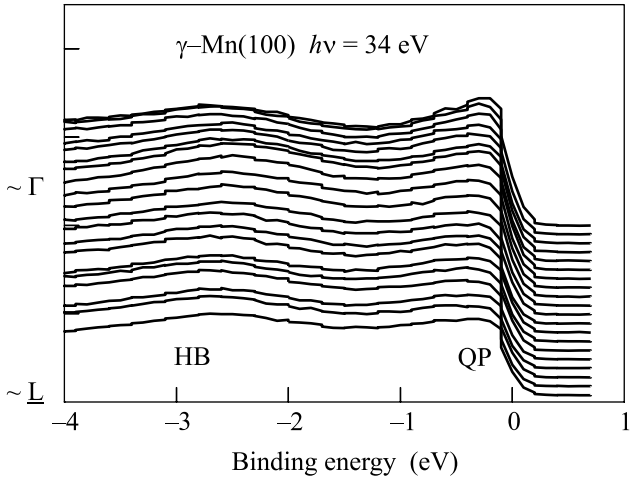


Fig.1. ARPES spectra of bulk-like γ-Mn (17 ML) taken at a photon energy of 34 eV for different electron emission angles corresponding approximately to $\mathbf{k}$-vectors between the Γ and the $L$ point in the Brillouin zone; binding energies are measured with respect to the Fermi energy. This should be compared to the negative energy parts of the calculated spectra in Fig.3

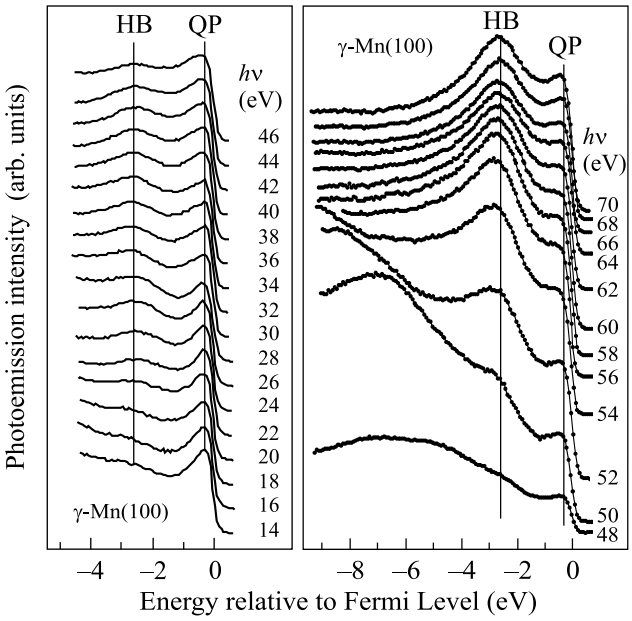


Fig.2. ARPES spectra taken in normal emission at photon energies of 14 to 70 eV. The lack of dispersion distinguishes γ-Mn from other transition metals. The spectra are normalized to the photon flux. Note that the spectral changes from 48 eV to 52 eV are due to resonant transitions between $3p$ and $3d$ states

To test this hypothesis we have carried out first principles (LDA+DMFT) calculations [19, 20] of the electronic structure of γ-Mn that include correlation effects in a local but fully dynamical approximation for

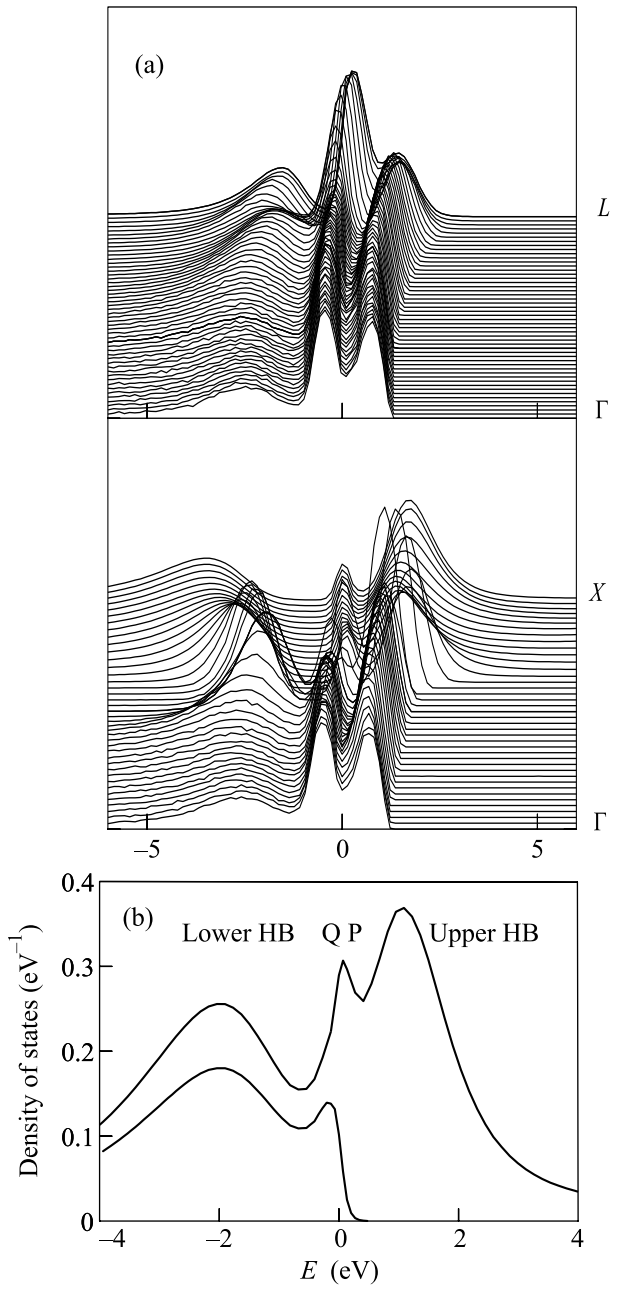


Fig.3. Spectra calculated within the LDA+DMFT approach: Upper panel : **k**-resolved density of states $A(\mathbf{k},\omega)$ [arbitrary units]. The different curves correspond to $k$-points between the Γ and the $L$-point and the Γ and the $X$-point respectively. Lower panel : Angle-integrated spectral function. The "three-peak structure" with the two broad Hubbard bands (HB) and a narrow quasiparticle (QP) Kondo resonance at the Fermi level (solid line) is typical of strongly correlated systems. The calculated angle-integrated photoemission spectrum (dashed line), i.e. the density of states multiplied with the Fermi function and broadened with the experimental resolution, shows reasonable agreement with the experimental spectra

the electron self-energy Σ, using the full Hamiltonian LDA+DMFT scheme described in [4] with U values between 3 and 5 eV and J=0.9 eV. Carrying out between 10 to 15 DMFT iterations with about $10^5$ Quantum Monte Carlo sweeps [21] allows us to obtain not only the local Green's function $G(\tau)$ but also highly accurate self-energies which can then be used for the computation of the **k**-resolved local Green's function

$$\hat{G}(\mathbf{k},\tau) = \frac{1}{\beta}\sum_n e^{-i\omega_n\tau}\left(i\omega_n + \mu - \hat{H}^{\mathrm{LDA}}(\mathbf{k}) - \hat{\Sigma}(i\omega_n)\right)^{-1}, \quad (1)$$

where $\omega_n$ are the Matsubara frequencies corresponding to the inverse temperature $\beta \sim 0.002\,\mathrm{K}^{-1}$, and $H^{\mathrm{LDA}}$ denotes an LDA-LMTO [22] spd-Hamiltonian corrected for double counting of the Coulomb energy of the $d$ states in the usual way [20]. Inversion of the spectral representations of the local Green's function and the dd-block of the **k**-resolved one by means of a Maximum Entropy scheme [23] yields the density of states (DOS) $\rho(\omega)$ and the spectral function $A(\mathbf{k},\omega)$. To our knowledge these calculations are the first ones that determine the **k**-dependence of the spectral density for a material with $d$-states from LDA+DMFT with a realistic five-band Coulomb vertex.

The results are shown in Fig.3, displaying the local density of states (b) and the **k**-resolved spectral functions $A(\mathbf{k},i\omega)$ for **k** points in the Γ−$L$ and Γ−$X$ directions respectively. In the negative energy part (that is for the occupied states) of all spectra two main peaks carry – for a given $k$-point – the main part of the spectral weight: a narrow quasi-particle (QP) feature near the Fermi level and a very broad Hubbard band (HB) (at about −2.4 eV). These features are shared between the experimental (Fig.1) and theoretical curves. The stronger dispersion of the (still very broad) low energy peak in the Γ−$X$ direction can be traced back to $d$-states that strongly hybridise with the $s$-band in that region of energy and **k** space. In the photoemission spectra these $s$-like bands are suppressed due to matrix element effects. Given the facts that (i) the experiments are done at a somewhat lower temperature than the calculations, that (ii) we do not take into account matrix elements for interpreting the photoemission data and that (iii) using the Maximum Entropy scheme for determining the spectral function, a quantity *not* directly measured within the Quantum Monte Carlo simulations, introduces a further approximation, the theoretical spectra agree reasonably well with the experimental data (Figs.1 and 2). In Fig.4 the Kohn-Sham eigenvalues taken from the LDA calculation are plotted. The absence of LDA bands in the energy region near $E_F$ carrying most of the spectral

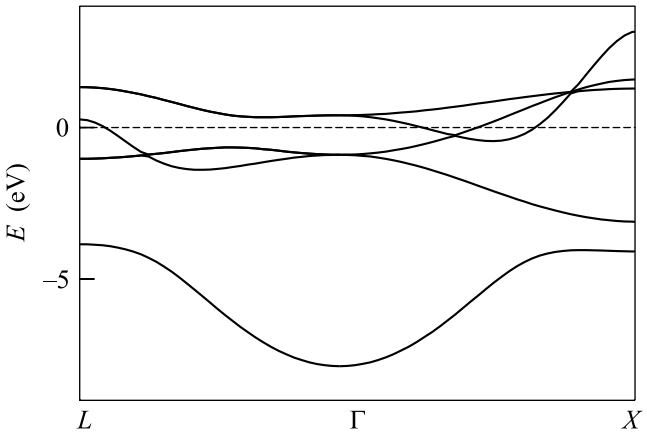


Fig.4. Band structure of $\gamma$-Mn as calculated within density functional theory within the local density approximation (LDA)

weight around the Γ-point is striking and underlines the necessity of a proper many body treatment as done in LDA+DMFT. Note that assuming antiferromagnetic order (of the type detailed below) would slightly shift the LDA bands. However, the antiferromagnetic LDA band structure displays a dispersion of more than 2 eV and could thus not explain the nondispersive photoemission feature.

The calculated (**k**-integrated and **k**-resolved) density of states curves (Fig.2) demonstrate a characteristic "three-peak structure", with two broad Hubbard bands and a narrow quasiparticle Kondo resonance at the Fermi level which is typical of strongly correlated electron systems [2]. The quasiparticle peak at the Fermi level and the lower Hubbard band are seen in the present ARPES spectra; in k-unresolved (BIS) measurements [24] a broad peak has been observed at 1.4 eV. To identify this peak with the upper Hubbard band (located at 1.2 eV in our calculations) one should prove the dispersionless nature of this peak. We have checked that all these incoherent features do not depend on the directions in **k**-space used in our calculations. For the above reasons we believe that $\gamma$-Mn belongs to the class of strongly correlated materials and that the ARPES data can be considered as the first observation of Hubbard bands in a transition metal.

The energy scale associated with the correlation effects that lead to the formation of the Hubbard bands ($\sim U$) is much larger than that of the magnetic interactions. Therefore the observed effects are not very sensitive to long-range magnetic order. We have carried out the electronic structure calculations for both the paramagnetic and the antiferromagnetic structure with wave vector $Q = (\pi,0,0)$, which is typical of $\gamma$-Mn-based alloys [25]. The magnetic ordering changes the electron spectrum little in comparison with the nonmagnetic case. However, in comparison with the results of standard band theory [12], the correlation effects stabilize the antiferromagnetic structure leading to a magnetic moment of about $2.9\,\mu_B$.

According to the present results, $\gamma$-Mn can be considered a unique case of a strongly correlated transition metal. An even larger correlation would transform the system to a Mott insulator where every atomic multiplet forms its own narrow but dispersive Hubbard band [1, 3]. On the other hand, in most metals correlations are small enough for the quasiparticles to be well-defined in the whole energy region and usual band theory gives a reasonable description of the energy dispersion. Note that the correlation strength and bandwidth have almost the same magnitude for all $3d$ metals. $\gamma$-Mn is probably an exceptional case among the transition elements due to the half-filled $d$-band and geometric frustrations in the fcc-structure.

In conclusion, our ARPES data for the $\gamma$-phase of manganese and their theoretical analysis by means of LDA+DMFT, an approach that accounts not only for band structure effects on the LDA level but also allows for a full description of local effects of strong Coulomb correlations, provide evidence for the formation of Hubbard bands in metallic manganese. This is a qualitatively new aspect in the physics of transition metals.

This research has been supported by grants of supercomputing time at NIC Jülich and IDRIS Orsay and by the Netherlands Organization for Scientific Research (NWO project #047-008-16).

* Present address: CPHT, Ecole Polytechnique, 91128 Palaiseau, France.

1. J. Hubbard, Proc. R. Soc. **A281**, 401 (1964).
2. A. Georges et al., Rev. Mod. Phys. **68**, 13 (1996).
3. N. F. Mott, *Metal-Insulator Transitions*, Taylor and Francis, London, 1974.
4. A. I. Lichtenstein, M. I. Katsnelson, and G. Kotliar, Phys. Rev. Lett. **87**, 67205 (2001).
5. P. Thiry et al., Phys. Rev. Lett. **43**, 82 (1979).
6. J. A. Knapp, F. J. Himpsel, and D. E. Eastman, Phys. Rev. **B9**, 4952 (1979).
7. S. Hüfner and G.K. Wertheim, Phys. Lett. **A51**, 299 (1975).
8. C. Guillot et al., Phys. Rev. Lett. **39**, 1632 (1977).
9. M. I. Katsnelson and A. I. Lichtenstein, J. Phys.: Condens. Matter **11**, 1037 (1999).
10. F. J. Himpsel, P. Heimann, and D. E. Eastman, J. Applied Phys. **52**, 1658 (1981).
11. N. E. Zein, Phys. Rev. **B52**, 11813 (1995).

12. V. L. Moruzzi, P. M. Marcus, and J. Kubler, Phys. Rev. **B39**, 6957 (1989).
13. A. F. Guillermet and G. Grimvall, Phys. Rev. **B40**, 1521 (1989).
14. B. Schirmer et al., Phys. Rev. **B60**, 5895 (1999).
15. S. D. Kevan, *Angle-resolved photoemission: Theory and current applications*, vol. **74**, Elsevier, Amsterdam, 1992.
16. O. Rader and W. Gudat, *Landolt-Börnstein*, New Series III, Vol. **23**, C2, Ed. A. Goldmann, Springer Verlag, Berlin, 1999.
17. D. J. Crockford, D. M. Bird, and M. W. Long, J. Phys.: Cond. Matt. **3**, 8665 (1991).
18. A. Georges and G. Kotliar, Phys. Rev. **B45**, 6479 (1992).
19. V. I. Anisimov et al., J. Phys.: Condens. Matter **9**, 7359 (1997).
20. A. I. Lichtenstein and M. I. Katsnelson, Phys. Rev. **B57**, 6884 (1998).
21. J. E. Hirsch and R. M. Fye, Phys. Rev. Lett. **56**, 2521 (1986).
22. O. K. Andersen, Phys. Rev. **B12**, 3060 (1975).
23. M. Jarrell and J. E. Gubernatis, Phys. Rep. **269**, 133 (1996).
24. W. Speier et al., Phys. Rev. **B30**, 6921 (1984).
25. R. S. Fishman and S. H. Liu, Phys. Rev. **B59**, 8681 (1999).